FRACTURE APERTURE MEASUREMENT AND CONSEQUENCES FOR GROUTING

J. Thörn
Division of GeoEngineering, Department of Civil and Environmental Engineering, Chalmers University of Technology, Sweden

Å. Fransson
Division of GeoEngineering, Department of Civil and Environmental Engineering, Chalmers University of Technology, Sweden

Summary

The hydraulic and the mechanical apertures of fractures and the relation between them are of interest for hydromechanical (HM) coupling and design of grouting works and reinforcement. The fracture geometry will influence **water inflow** to underground constructions, **penetrability** and **penetration length** of grout and **mechanical properties** of the fracture. This paper aims at presenting fracture geometry measurements on one fracture sample and to use this as a basis for a discussion on consequences for grouting.

To measure surface topography of the two sides of a rock core fracture sample from the TASS-tunnel, Äspö HRL (Sample and sampling described in Ericsson et al. 2009) commercial equipment for stereo photogrammetry was used. Prior to scanning each surface, their relative positions were determined at 1.0 MPa confining pressure. The procedure enables a computer comparison between the surfaces, rendering an aperture map for the specific confining pressure. The measured surface geometry provided a data set that was put in the context of hydraulics, mechanics and hydromechanics. Comments on how the applications inflow, grout spread, fracture deformation and block stability can be related to the fracture geometry are given.

1   Introduction

The mechanical and hydraulic behaviour of a fracture is dependent on the fracture void geometry and the boundary conditions (e.g. stresses and pore pressure) in which the fracture is situated. Fracture void geometry relates to a number of properties, Hakami (1995) mentions eight such properties: *aperture*, i.e. the distance between the surfaces; the *contact area* between the surfaces; the *roughness* and *matedness* of the surfaces, i.e. how coarse the surfaces are and how well they fit together; the *spatial correlation*; presence of *channelling*, i.e. continuous, wider paths that may transmit water; *tortuosity*,

i.e. un-straightness of flow paths and the *stiffness* across the surfaces, i.e. the measure of the stress needed to bring the surfaces one length-unit closer to each other. The presence of mineral precipitates or gouge products in the void could affect the properties in various ways.

Knowledge of the fracture void space and how it has come to be is beneficial for predicting the behaviour of a fracture for tunnelling applications, such as grouting. The aim of the current paper was to measure the aperture at a known stress situation and compare it with cubic law hydraulic aperture, established from previous hydraulic testing and to put the results into the context of possible consequences for grouting.

The method chapter starts with a section on the setup for surface geometry measurement, followed by a description of how the resulting data was processed. Thereafter the aperture of the sample is presented. The discussion chapter contains a section on the measurements and what they are and are not. Further, the consequences for grouting of the specific fracture geometry are addressed, as well as comments on grouting in a more general sense.

2 Method
2.1 Measurement single fracture
In order to measure the mechanical aperture at a known stress situation that was similar to the situation at previously conducted flow experiments (Ericsson et al. 2009; Thörn et al. 2013; Thörn 2012), the core (PS0039061) was put under a biaxial pressure in a permeameter. The permeameter cell had to be modified, enabling a visible top surface of the sample. A series of photographs were taken on the top surface of the core, see Figure 1 and Figure 2-1.

The photographs were processed by computer software that utilized code markings and dots that were placed on the surface for determining the relative positions of the sample halves, putting them in a common coordinate system. When this was done, the core was removed from the cell, and split. The dots on the upper surface of the core were supplemented with dots on the fracture surface (see green dots on the "computer screen" in Figure 2).

Photographing was conducted again, one core half at a time (Figure 2-2) before scanning the surface geometry of each half (Figure 2-3). The dots that were attached to the sample before the photographing for enabling construction of a coordinate system were identified by the scanning software, which aligned the scanned surfaces into the established coordinate system (Figure 2-3). The point clouds obtained from the scans were converted to meshes. The meshes of the halves were then compared, and a high

resolution map of the distance between the surfaces, i.e. the mechanical aperture, was obtained (Figure 2-4 and Figure 3).
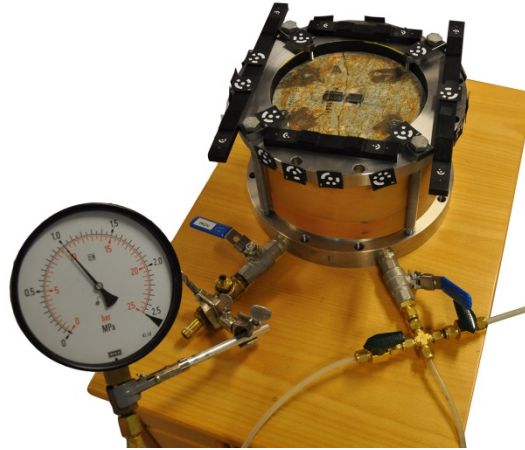

Figure 1: Sample pressurized to 1.0 MPa with top surface free, ready for the first step of determining the relative positions of the sample halves in a common coordinate system. See also Figure 2-1.

2.2 Data processing

Aperture data was analysed as suggested by Zimmerman and Bodvarsson, (1996), Eq. 1, where b [μm] is the hydraulic aperture, a [μm] is the arithmetic mean of the mechanical aperture, σ [μm] its standard deviation and c [-] is the proportion of contact area of the surfaces.

$$b^3 = \langle a \rangle^3 \left[1 - \frac{1.5\sigma_a^2}{\langle a \rangle^2} \right](1 - 2c) \qquad \text{Eq. 1}$$

This hydraulic aperture is compared to an estimate of hydraulic aperture from permeameter experiments evaluated with the common parallel plate model referred to as the Cubic law (Eq. 2). Eq. 2 includes a transmissivity from Darcy's law (Eq. 3) where Q [m^3/s] is the flow, L [m] is flow length, W [m] is flow width. In addition, g [9.81 m/s^2] is acceleration due to gravity, μ_w [1.003 mPas] is viscosity of water and ρ_w [998.2 kg/m^3] is density of water.

$$b = \sqrt[3]{\frac{12 \cdot \mu_w \cdot T}{\rho_w \cdot g}} \qquad \text{Eq. 2}$$

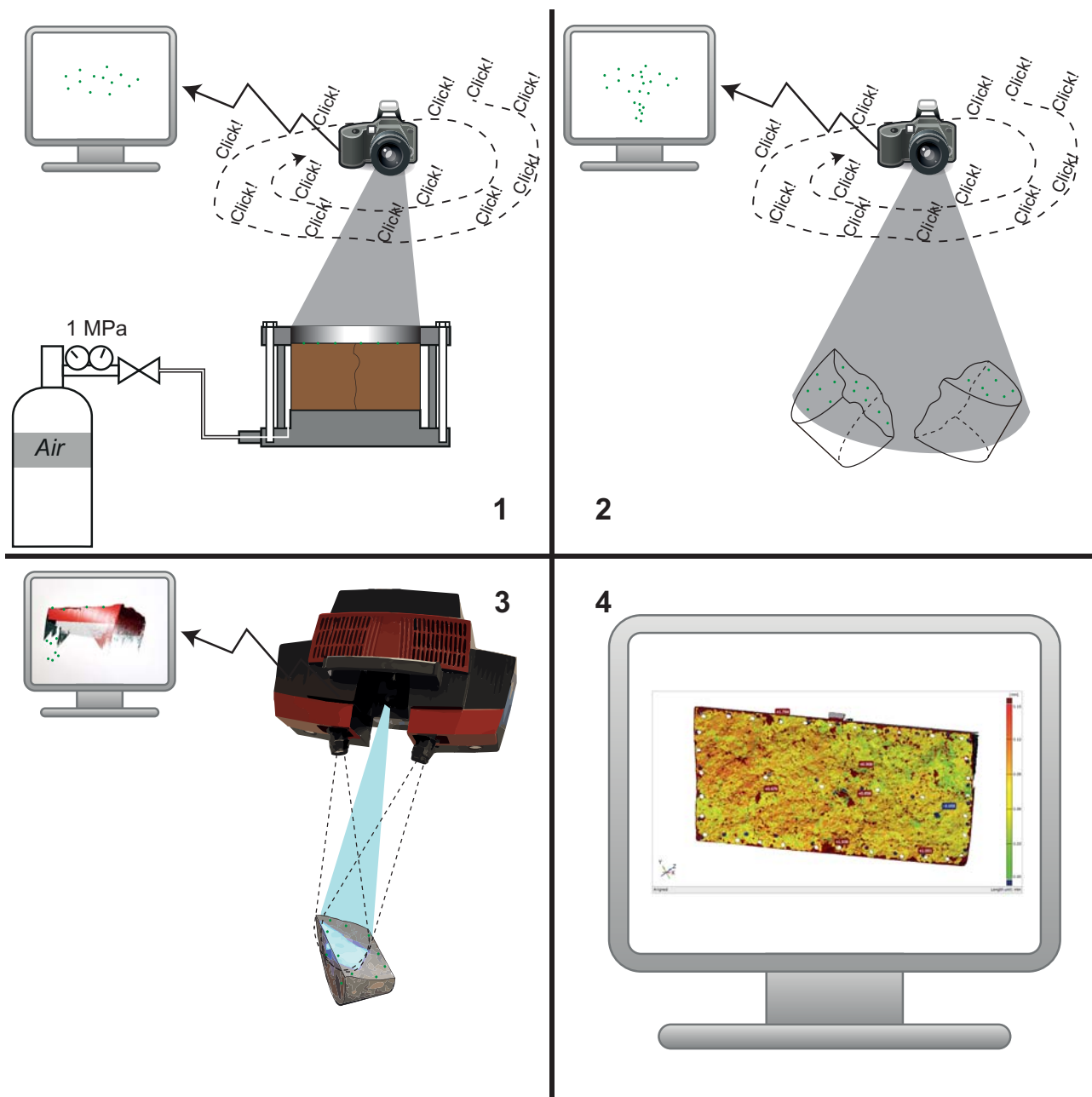$$T = \frac{Q \cdot L}{dh \cdot W} \qquad \text{Eq. 3}$$

Figure 2: Sequence for scanning and generating an aperture map. Note the green coordinate dots on the sample and correspondingly on the computer screen (dots are black/white in reality). Step 1 captures the relative positions of the fracture halves when under a defined pressure, as seen on the top surface. Step 2 adds the dots on the fracture surface into the same coordinate system so that surfaces can be aligned. In step 3 the coordinate dots are supplemented by a precise surface scan, including both dots and the rough fracture surface in between. In step 4 the distances between points in the scanned halves are calculated, rendering an aperture map, see further Figure 3.

3   Aperture of sample

The aperture map of PS0039061 at 1.0 MPa can be seen in Figure 3. Calculations were made on a subsection of the sample area, excluding the holes in the meshes (blue or white) that originate from the coordinate dots on the sample halves. By means of Eq. 1 the hydraulic aperture was estimated to 66 μm, which is close to 73 μm: the aperture from previous permeameter testing, evaluated according to Eq. 2 (Thörn et al. 2013; Thörn 2012).

The parameters in Eq. 1; values of the arithmetic mean aperture, a = 93 μm and its standard deviation, σ = 60 μm was obtained from a built-in statistics tool in the analysis software that comes with the scanning hardware. The concept of contact is scale dependent in its definition, and a threshold value is needed for defining contact and calculating contact area, c (Hakami 1995). A threshold of 10 μm was used for contact, and rendered c ≈ 0.7%. 10 μm may seem much in relation to the aperture, but assigning c = 0% only increased the output hydraulic aperture by a third of a micron.
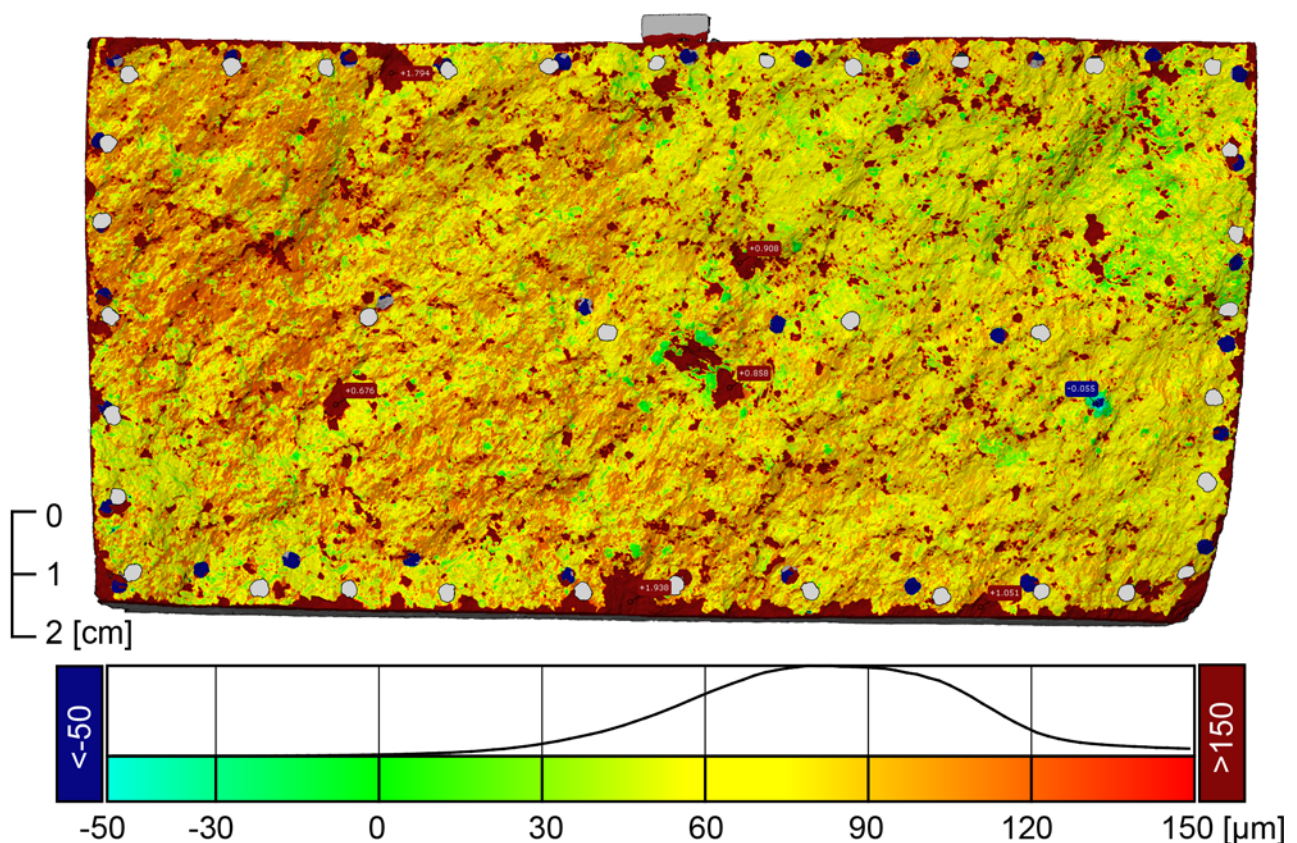

Figure 3: Aperture map of PS0039061 from the scan setup at 1.0 MPa confining pressure. Histogram of the apertures is included in the scale bar. The aperture map shows an open fracture with few contact points i.e. resembles a parallel plate model where radial (2D) flow is expected.

4 Discussion

4.1 Measurements

The measurement hardware and analysis software is able to deliver output accurate down to a few microns. For fractures that are groutable with cement this resolution is considered sufficient. The method based on scanning is deemed robust and result in similar aperture values as the previous permeameter testing of the sample. Hydraulic aperture from scanning of the sample, calculated according to Eq. 1 match the cubic law aperture from previous permeameter measurements well. The main thing to bear in mind is that the tested conditions is not necessarily the same as the in situ conditions, e.g. with respect to the positions and possible rotation of the sample halves relative each other; the effect of boundaries, e.g. the large scale appearance of the fracture and an appropriate level of stress. Therefore the results should be used as "a fracture that looks like this in situ would behave…" rather than "The laboratory testing of *this* fracture describes *its* in situ properties".

4.2 Geological history, geometry, hydraulics, mechanics and hydromechanics

A schematic diagram of the world of a fracture in crystalline rock during construction works is found in Figure 4. The current fracture geometry is a product of the way it was formed, and the processes it has been through since then (e.g. reactivations; faulting with gouge production; mineral precipitation). This together with the current boundary conditions, i.e. the rock stresses, pore pressure and interaction with the rest of the fracture system, governs the behaviour of the fracture when disturbed by grouting or excavation.

Traditionally the behaviour is described either in terms of hydraulics or rock mechanics, but a description that couples hydraulic and rock mechanical behaviour to the geological setting and geometry (exclamation mark in Figure 4) is beneficial. Incorporating knowledge about the geology and geometry enables narrowing the range of possible fracture geometries and corresponding behaviour for a given application. An example is that a joint (i.e. mated or unsheared) with an orientation such that it is in a compressional stress regime can be expected to have a small hydraulic aperture, small inflow and high stiffness. An unmated fracture like the one presented in Figure 3 has a larger aperture and would only exist under a low compressive stress since permanent deformation and crushing occur at higher stress. The behaviour of this particular fracture is further discussed in section 4.3.
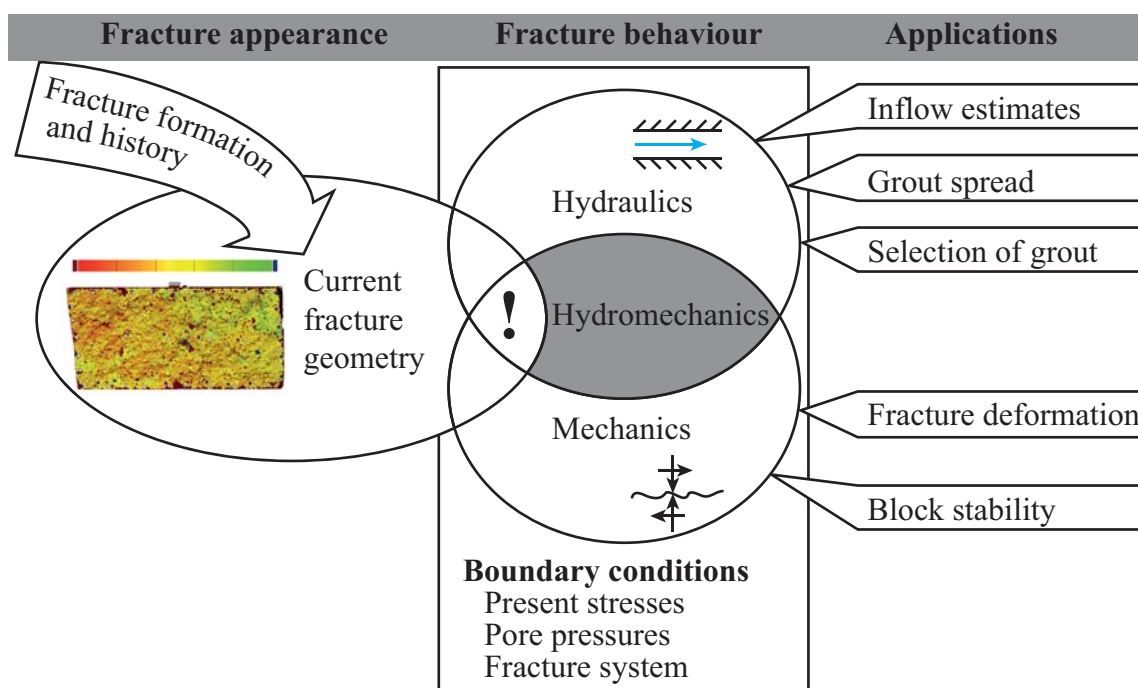
Figure 4: A schematic diagram describing fracture geometry, behaviour and some examples on applications: inflow, grout spread, selection of grout, fracture deformation and block stability.

4.3 Applications, relating to a single open fracture

The cubic law (eq. 2) provides a straightforward estimate of the hydraulic aperture, which can be used for selecting a grout that is suitable for the aperture at hand, e.g. as presented in Fransson (2009). If a too coarse-grained grout is selected, the penetration is significantly reduced, see e.g. Gustafson et al. (2009). A rule of thumb for the *penetrability* is that the d_{95} of the grout grains must be less than a third of the hydraulic aperture.

The *maximum penetration length* or grout spread of a cementitious grout (Bingham fluid), (see e.g. Hässler (1991) or Gustafson and Stille (2005)) as Eq. 4, where Δp is the grouting overpressure, b is the hydraulic aperture and τ_0 is the yield strength of the grout.

$$I_{max} = \frac{\Delta p \cdot b}{2\tau_0}$$
Eq. 4

For comparison, the penetration of Silica Sol (Newtonian fluid) can be found in Funehag and Gustafson (2008a, b). It is evident from Eq. 4 that the grout spread is dependent on the interaction between rock (b), grout mix (τ_0) and the grouting procedure (Δp).

Under *hydromechanical* permeameter testing the sample showed similarities with the conceptual description of increasing stiffness but limited change of hydraulic aperture. Therefore the effect on tortuosity is small and the fracture can be regarded as "as open as before" Two other types of fracture behaviour is also identified in (Thörn 2013; Thörn et al. 2013), also relating to the matedness of the fracture surfaces. These are a) a small aperture with high stiffness growth, needing fine-grouting agent; and b) an intermediate where the hydraulic aperture is changed with changed mechanical load across the fracture.

For a well-mated fracture the contact area is likely to be larger, or at least with smaller spacing between contact points. A larger area in contact relates to a higher stiffness. Also, increased contact area reduces the hydraulic aperture (Eq. 1) and the penetrability, and the fracture eventually approaches the percolation limit, where the large area in contact prevents the water or grout from finding a continuous pathway through the fracture.

4.4 Applications, relating to fracture system

The behaviour of the individual fracture is influenced by the fracture system, stresses and pore pressures. Figure 5 presents permeability structures for host rock (hydraulic rock domains) and fault zones (hydraulic conductor domains). These descriptions can serve as a basis when discussing the hydromechanical behaviour of a fractured rock mass.
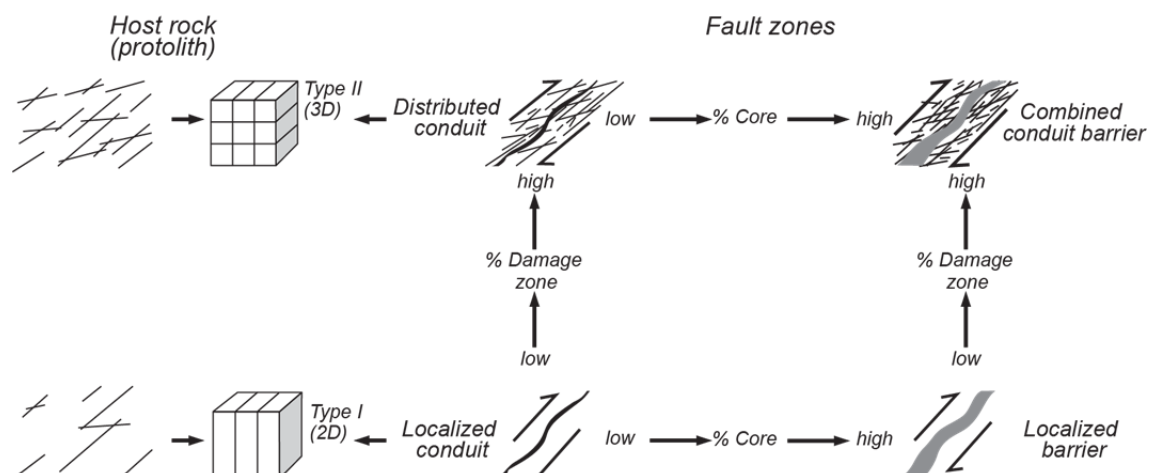

Figure 5: Conceptual scheme for permeability structures in host rock, hydraulic rock domain (Fransson and Hernqvist 2010) and in deformation (fault) zones, hydraulic conductor domains (modified from Caine et al. 1996).

From a *mechanical* or *hydromechanical* perspective, grouting near tunnel walls, inside the perturbed stress field require extra attention regarding the stability and risk for

jacking of fractures. The same applies to grouting in surficial rock, e.g. grout curtains under dams or engineered foundations (see e.g. Johansson 2009; Bondarchuk 2012). Post-grouting work for dam restoration therefore requires special attention in terms of permissible grout pressures. This is particularly true for densely fractured rock of Type II, in deformation zones or in the excavation damaged zone (EDZ). In tunnelling, rock movements due to excavation may damage the pre-grouted zone. In such cases it may be beneficial to apply measures that handle both support/stability and waterproofing, such as local cast lining. But essential for the success is that both hydraulic and rock mechanical design is synchronized and non-competitive.

Considering a grouting design where more fractures than the least stiff needs to be sealed in order to fulfil the inflow requirements, jacking can result in undesired effects. Grout penetration occurs simultaneously in all fractures that the grout is able to penetrate, but with different velocity for different apertures (fast spread in large fractures). If the pressure is high enough for jacking, high aperture and low stiffness fractures in certain alignment to the stress field will be the first to experience jacking. The spread in these fractures will accelerate, but the sealing needed to fulfil the requirements in the design, does not benefit from it. In a favourable case, jacking can be a waste of grout. In worse cases fractures that need to be sealed are temporarily or permanently closed somewhat, which affect penetration. High grout spread rates may also affect the surroundings, e.g. reaching the surface, or contributing to opening of new flow paths.

The previous discussion has been focused on reasoning and research about fracture appearance and behaviour, the last paragraphs are dedicated to some field experiences. The rock stresses, often roughly proportional to the depth of a tunnel to be grouted influence the grouting results. Fransson et al. (2010) compare grouting results and hydraulic testing for two tunnels (The Nygård tunnel, shallow train tunnel in SW Sweden, and the deep TASS tunnel in Äspö HRL) and evaluate the pumping data in terms of deformation and stiffness behaviour of the intersected fractures. The Nygård tunnel was found to have low fracture stiffness and consequently larger fracture deformations than in the more highly stressed TASS tunnel.

Hydromechanical effects due to grouting has also been identified at e.g. Botniabanan in Sweden (Gothäll and Stille 2009), where a change in grouting pressure during grouting resulted in a larger than expected increase in grout flow. In addition, the importance of the in-situ stress is discussed by Beitnes (2005) in a study of the post-excavation grouting at Romeriksporten, Norway.

5   Conclusions

The measured surface geometry provided a data set that was put in the context of hydraulics, mechanics and hydromechanics. In addition suggestions were given on how the applications inflow, grout spread, fracture deformation and block stability can be related to the geometry. This can be used for narrowing the sample space in which a fracture can be expected to exist. The following conclusions are drawn:

- The geometry of the scanned sample from the TASS tunnel provide a good fit between estimates of hydraulic aperture from the cubic law and the Zimmerman & Bodvarsson equation (Eq. 1). Low contact area corresponds to a low stiffness and combined with low standard deviation of aperture the sample resemble the plane parallel cubic law model.
- The aperture and geometry of the scanned fracture suggest that ordinary grouting cement such as *Cementa Injektering 30* is close to the rule of thumb of d95 < aperture/3 and may not penetrate properly. But finer ground cement or other fine-sealing product can be expected to penetrate in a good 2D fashion.
- Higher stress across a fracture results in larger contact area, lower hydraulic aperture and reduced grout penetrability.
- Deformations and ultimately jacking of fractures may result in adverse effects in the grouted rock mass and reduced control of the grouting progress.
- Monitoring of grouting and hydraulic testing can be used to give indications of movements in the rock mass, which can be developed to help in determining the stability and designing the support of a tunnel.
- For e.g. deformation zones where both waterproofing and stability measures may face challenges, a collaborative design work can come up with measures likely to effectively deal with both sealing and stability issues.
- An expanded study and scanning campaign may be able to support a generic model covering a larger aperture range and genesis of fractures.

Acknowledgments

References

Beitnes A (2005) Lessons to be learned from Romeriksporten. Tunnels and Tunnelling International vol. 37 (6, June):pp. 36-38.

Bondarchuk A (2012) Rock mass behavior under hydropower embankment dams with focus on fracture erosion and rock mass stability. Ph.D. Thesis, Luleå University of Technology, Luleå Sweden.

Caine JS, Evans JP, Forster CB (1996) Fault zone architecture and permeability structure. Geology 24 (11):1025-1028.

Ericsson LO, Brinkhoff P, Gustafson G, Kvartsberg S (2009) Hydraulic Features of the Excavation Disturbed Zone - Laboratory investigations of samples taken from the Q- and S-tunnels at Äspö HRL. R-09-45. Swedish Nuclear Fuel and Waste Management Co, Stockholm, Sweden.

Fransson Å (2009) Selection of grouting material based on a fracture hydraulic aperture assessment. Paper presented at the Proceedings of the Nordic symposium of rock grouting, 5th November, Helsinki, Finland

Fransson Å, Hernqvist L (2010) Geology, water inflow prognosis and grout selection for tunnel sealing: Case studies from two tunnels in hard rock, Sweden. Paper presented at the ITA-AITES World Tunnel Congress. May 17-19, Vancouver, Canada

Fransson Å, Tsang CF, Rutqvist J, Gustafson G (2010) Estimation of deformation and stiffness of fractures close to tunnels using data from single-hole hydraulic testing and grouting. International Journal of Rock Mechanics and Mining Sciences 47 (6):887-893.

Funehag J, Gustafson G (2008a) Design of grouting with silica sol in hard rock – New design criteria tested in the field, Part II. Tunnelling and Underground Space Technology 23 (1):9-17.

Funehag J, Gustafson G (2008b) Design of grouting with silica sol in hard rock – New methods for calculation of penetration length, Part I. Tunnelling and Underground Space Technology 23 (1):1-8.

Gothäll R, Stille H (2009) Fracture dilation during grouting. Tunnelling and Underground Space Technology 24 (2):126-135.

Gustafson G, Fransson Å, Butron C, Hernqvist L (2009) Effective fracture aperture for grout penetration. Paper presented at the Nordic symposium of rock grouting, 5th November, Helsinki, Finland

Gustafson G, Stille H (2005) Stop criteria for cement grouting. Felsbau : Zeitschrift für Geomechanik und Ingenieurgeologie im Bauwesen und Bergbau 25:3:62-68.

Hakami E (1995) Aperture distribution of rock fractures. Ph.D. Thesis, Royal Institute of Technology, Stockholm, Sweden

Hässler L (1991) Grouting of rock : simulation and classification. Ph.D. Thesis, Royal Institute of Technology, Stockholm, Sweden

Johansson F (2009) Shear strength of unfilled and rough rock joints in sliding stability analyses of concrete dams. Ph.D Thesis, Royal Institute of Technology, Stockholm

Thörn J (2012) Coupling between changes in hydraulic and mechanical aperture: A laboratory study on rock cores. Report 2012:9. Chalmers University of Technology, Gothenburg, Sweden.

Thörn J (2013) Hydromechanical Behaviour of Fractures Close to Tunnels in Crystalline Rock. Licentiate thesis, Chalmers University of Technology, Gothenburg, Sweden

Thörn J, Ericsson LO, Fransson Å (2013) Hydraulic and Hydromechanical Laboratory Testing of Large Crystalline Rock Cores. Submitted to Rock Mechanics and Rock Engineering.

Zimmerman RW, Bodvarsson GS (1996) Hydraulic conductivity of rock fractures. Transport in Porous Media 23 (1):1-30.